

Couple stress and poro-elasticity effects on squeeze film

O. S. T. GBEHE, M. NABHANI, M. EL KHLIFI

Hassan II University of Casablanca, Faculty of Sciences and Techniques,
PO Box146, 20650 Mohammedia, Morocco, mohamed_elkhlifi@yahoo.fr

Abstract

This study deals with a numerical simulation of couple stress and poro-elasticity effects on hydrodynamic performances of squeeze film between infinitely long parallel plates. The lower plate is an elastic porous matrix saturated by a fluid film and its poro-elasticity is taken into account by the means of homogenization method. The modified Reynolds equation in the fluid film and the homogenized equations in the poro-elastic plate, discretized by finite differences method, are coupled using sequential algorithm and solved iteratively using Gauss-Seidel over-relaxation method.

Keywords: *couple stress; poro-elasticity; squeeze film; numerical simulation.*

1. Introduction

The technology of porous squeeze films is widely used in industry and biomechanics. The studies of porous squeeze films focus traditionally on rigid porous materials [1 - 3]. The study of Gbehe *et al.* [4] take into account the poro-elasticity effects of a porous squeeze film by the means of homogenization method [5]. In this latter study the fluid film is considered Newtonian. In realities, the Newtonian fluid is doped by suspended particles and thus its rheological behavior is non-Newtonian. The present paper deals with a numerical simulation of poro-elastic squeeze film considering non-Newtonian effects based on The Stokes couple stress theory [6]. The poro-elasticity of the porous plate is taken into account by the homogenization method.

2. Problem definition and governing equations

Consider two parallel infinitely long flat plates of length L immersed in a non-Newtonian lubricant (Figure 1). The lower plate of thickness H is fixed and poro-elastic. The upper plate, located by $g(t)$ and supporting a constant load W_0 , is rigid and has a squeezing movement of instantaneous velocity $-dg/dt$.

The lubricant between the two flat plates is modelled as an incompressible Stokes couple stress fluid [6]. The flow is laminar and axisymmetric. Using the thin film assumption in absence of body forces and neglecting inertia effects into the fluid film, the continuity and motion equations in Cartesian coordinates read:

$$\frac{\partial v_1}{\partial x_1} + \frac{\partial v_2}{\partial x_2} = 0 \quad (1)$$

$$\frac{\partial p}{\partial x_2} = 0 \quad (2)$$

$$\frac{1}{\mu} \frac{\partial p}{\partial x_1} = \frac{\partial^2 v_1}{\partial x_2^2} - l^2 \frac{\partial^4 v_1}{\partial x_2^4} \quad (3)$$

where μ , p , v_1 and v_2 are respectively the dynamic viscosity, the pressure, the components of fluid velocity

vector in x_1 and x_2 directions respectively. $l = \sqrt{\frac{\eta}{\mu}}$ is the

couple stress parameter, where η represents a material constant responsible for the couple stress fluid property.

Integrating the momentum equations (3) using the no-slip condition and no couple stress on the upper plate and the slip velocity and no couple stress on the film – poro-elastic plate interface, the velocity component u_1 is obtained. Integrating the continuity equation (1) across the fluid film with respect to x_2 , the modified Reynolds equation is then derived:

$$\frac{\partial}{\partial x_1} \left[G(h,l) \frac{\partial p}{\partial x_1} \right] = 6\mu \frac{\partial}{\partial x_1} \left[\frac{U_b h}{2} \right] + 12\mu \frac{dg}{dt} - 12\mu v_2^* \quad (4)$$

where $G(h,l) = h^3 - 12hl^2 + 24l^3 \tanh\left(\frac{h}{2l}\right)$, v_2^* is the fluid velocity in x_2 direction at the film – poro-elastic plate interface and U_b is the Beavers-Joseph slip velocity [7] given for couple stress fluid by:

$$U_b = -\frac{k}{2\mu} \frac{\partial p}{\partial x_1} \left[\left(\frac{\sigma^2 + 2\alpha\sigma}{1 + \alpha\sigma} \right) - \frac{2hl}{k(1 + \alpha\sigma)} \tanh\left(\frac{h}{2l}\right) \right] \quad (5)$$

where $\sigma = \frac{h}{\sqrt{k}}$, k is the constant permeability of the poro-elastic plate.

h is the total fluid film thickness is given by:

$$h = g(t) + \delta \quad (6)$$

δ is the film – poro-elastic plate interface deflection.

The poro-elastic plate is considered homogenous, isotropic and composed of periodically reproduced elementary cell. The elementary cell, of length l and width e , is composed of solid matrix domain and pore domain saturated by the fluid film. The solid matrix is supposed to be elastic and its deformation is considered small. The suspended particles into the fluid film are assumed large and do not penetrate into the poro-elastic plate. Thus, the fluid film saturating the pore domain is Newtonian such as the study of Gbehe *et al.* [4]. Due to the assumption of scale separation, the unknown fields are functions of two independent space variables: macroscopic space variables (x_1, x_2) describing the poro-elastic plate and microscopic space variables (y_1, y_2) describing the elementary cell. The macroscopic equations within the poro-elastic plate, obtained by the use of homogenization technique [4], are:

$$\left\langle \begin{matrix} \rightarrow 0 \\ v_f \end{matrix} \right\rangle = -\frac{k}{\mu} \nabla_x p_f^0 \quad (7)$$

$$\frac{\partial p_f^0}{\partial x_1} + \frac{\partial p_f^0}{\partial x_2} = 0 \quad (8)$$

$$\nabla_x \left[C_{ijmn}^{eff} E_{mn} \left(\begin{matrix} \rightarrow 0 \\ u_s \end{matrix} \right) - \alpha_{ij} p_f^0 \right] = \vec{0} \quad (9)$$

where k , C_{ijmn}^{eff} , α_{ij} and $E_{mn} \left(\begin{matrix} \rightarrow 0 \\ u_s \end{matrix} \right)$ is a constant permeability of the poro-elastic plate, the effective elastic stiffness tensor, the Biot effective stress coefficient tensor and the macroscopic strain tensor. The equations (11) and (12) are respectively the Darcy's law and the Laplace equation and are defined into the fluid part. The equation (13) represents the equilibrium equation and is defined into the solid part. This macroscopic equilibrium equation depends of two microscopic displacement vectors solutions of microscopic equilibrium equations on the elementary cell [4].

The definitive partial differential equations in the fluid film (4) and the poro-elastic plate (11 – 13) are discretized by the finite difference method and the obtained algebraic equations are solved using the iterative Gauss-Seidel method. The coupled problem, film – poro-elastic plate, is solved using a sequential coupling algorithm based on fixed point technique.

3. Results and discussions

To examine the coupled effects of couple stress on the poro-elastic squeeze performances, the numerical results are presented and analyzed in the following for different couple stress parameter $\bar{l} = \frac{l}{h_0}$ and fixed permeability

parameter $\bar{k} = \frac{kH}{h_0^3}$ and flexibility parameter

$$\bar{C} = \frac{H(1+\nu)(1-2\nu)W_0}{h_0 E(1-\nu)L}$$

values. h_0 , ν and E are respectively the initial fluid film thickness, the Poisson ratio and the Young modulus.

Figure 2 shows the effects of couple stress on dimensionless load capacity for a poro-elastic plate. Due to the upper plate acceleration, the dimensionless load capacity increases with dimensionless time during initial stage of squeeze for all considered dimensionless couple stress parameter values. Then it decreases sharply and becomes almost constant at the end of the squeeze. Moreover, it's shown that the load capacity increases with the couple stress parameter during the initial stage of squeeze and then has no more effect. This rise of the load capacity is due to the influence of suspended particles into the lubricant which resist and oppose to the lubricant fluid motion and has as consequence the increase of pressure. This effect decelerates the upper plate motion and thus reduces its inertial force, which decreases the load capacity to balance the upper plate inertia.

Figure 3 presents the variation of friction coefficient as function of dimensionless time for different values of dimensionless couple stress parameter. The decrease of friction coefficient with time for all dimensionless couple stress parameter values is observed. During the initial stage of squeeze, the friction coefficient coincides for all dimensionless couple stress parameter value. However, it's then observed that the presence of suspended particles into the film fluid generates a greater friction coefficient compared to Newtonian fluid because of a higher value of the 'apparent' viscosity. This result is consistent with the variation of the load capacity presented in figure 1.

4. Conclusion

This paper deals with the couple stress and poro-elasticity effects on hydrodynamic performances of squeeze films. The lubricant in the fluid film region is modelled by the Stokes theory. The poro-elasticity effect into the poro-elastic plate saturated is taken into account by the homogenization method. According to the numerical results, due to the presence of suspended particles into the fluid film which decelerate the fluid film flow, the load capacity and the friction coefficient increases during the squeeze process.

References

- [1] PRK Murti, *Squeeze films in porous circular disks*, Wear 23(3) (1973) pp 283 - 289.
- [2] EM Sparrow, GS Beavers, IT Hwang, *Effect of velocity slip on porous-walled squeeze films*, ASME Jour. of Lubr. Tech. 94(3) (1972) pp 260 - 264.
- [3] AA Elsharkawy, MN Nassar, *Hydrodynamic lubrication of squeeze-film porous bearings*, Acta Mechanica 118(1) (1996) pp 121 - 134.
- [4] OST Gbehe, M El Khelifi, M Nabhani, B Bou-Saïd , *Numerical modeling of poro-elasticity effects on squeeze film of parallel plates using homogenization method*, Tribology International 102 (2016) pp 70 - 78.
- [5] E Sanchez-Palencia, *Non-Homogeneous Media and Vibration Theory*, Springer-Verlag, Heidelberg, 1980.
- [6] VK Stokes, *Couples Stresses in Fluids*, Phys Fluids 9(9) (1966) pp 1709 - 1715.
- [7] GS Beavers, DD Joseph, *Boundary conditions at a naturally permeable wall*, Journal of Fluid Mechanics 30(1) (1967) pp 197 - 207.

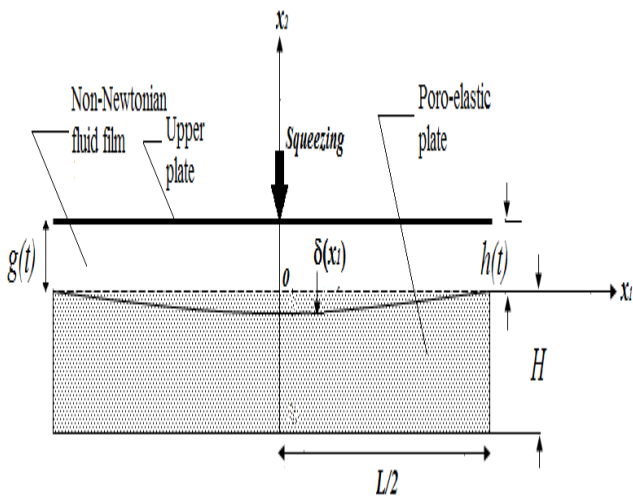


Figure 1: Squeeze film geometrical configuration

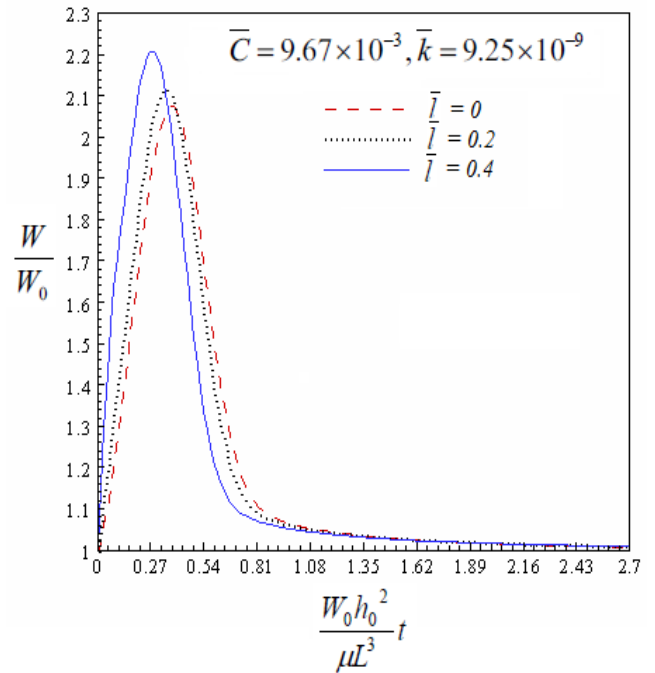


Figure 2: Variation of dimensionless load capacity as function of dimensionless time for different dimensionless couple stress parameter \bar{l}

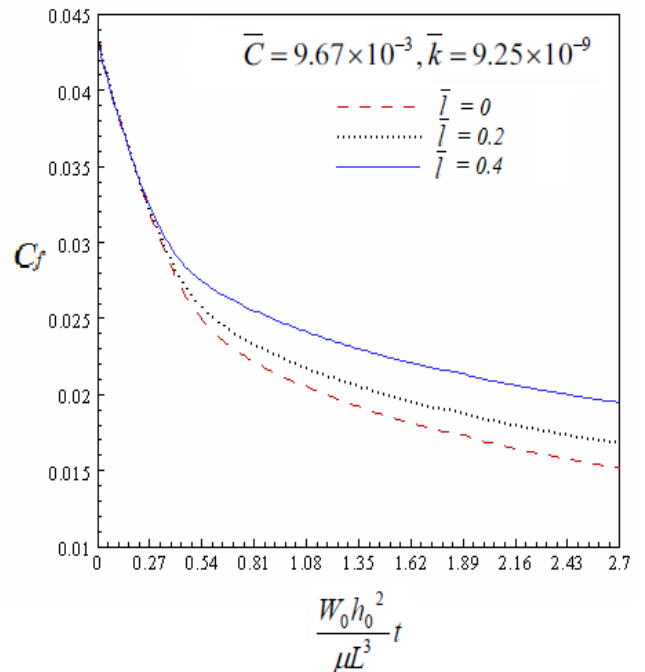


Figure 3: Variation of friction coefficient as function of dimensionless time for different dimensionless couple stress parameter \bar{l}